Materials Physics and Mechanics. 2022;50(1): 1-19
Research article
http://dx.doi.org/10.18149/MPM.5012022_1

Submitted: September 25, 2021
Approved: May 23, 2022
Accepted: June 24, 2022

Dispersion analysis of electrically actuated hygro-magneto-thermo-flexo electric nanobeam embedded on silica aerogel foundation

R. Selvamani[1]✉, L. Rubine[1], J. Rexy[1], F. Ebrahimi[2]

[1]Department of Mathematics, Karunya Institute of Technology and Sciences, Coimbatore-641114, Tamilnadu, India

[2]Department of Mechanical Engineering, Imam Khomieni International University, Qazvin34148-96818, Iran

✉ selvam1729@gmail.com

Abstract. This paper accesses the performance of applied electric voltage in a hygro thermo magneto flexo electric nanobeams embedded on a silica aerogel foundation based on nonlocal elasticity theory. Higher-order refined beam theory via Hamilton's principle is utilized to arrive at the governing equations of nonlocal nanobeams and solved by an analytical solution. A parametric study is presented to analyze the effect of the applied electric voltage on dimensionless deflection via nonlocal parameters, slenderness, moisture constant, critical temperature, and foundation constants. It is found that physical variants and beam geometrical parameters have significant effects on the dimensionless deflection of nanoscale beams. The accuracy and efficiency of the presented model are verified by comparing the results with that of published research. A good agreement has arrived.
Keywords: applied voltage, hygro thermo magnetic effect, flexoelectric nanobeam, nonlocal elasticity, refined beam theory, silica aerogel foundation

Acknowledgements. *No external funding was received for this study.*

Citation: Selvamani R, Rubine L, Rexy J, Ebrahimi F. Dispersion analysis of electrically actuated hygro-magneto-thermo-flexo electric nano beam embedded on silica aerogel foundation. *Materials Physics and Mechanics*. 2022;50(1): 1-19. DOI: 10.18149/MPM.5012022_1.

1. Introduction

Structural monitoring of nanobeams, nanoplates, and nanomembranes are recent novel field for many researchers due to their improvement of the quality properties. The classical continuum theory is aptly practical in the mechanical behavior of the macroscopic structures, but it is improperly for the size effect on the mechanical treatments on micro or nanoscale structures. Nevertheless, the classical continuum theory needs to be extended to factor in the nanoscale effects. The prime magneto-electro-elastic (MEE) was used in the 1970s, and MEE composite consisting of the piezoelectric and piezo magnetic phase was discovered this year. Van den Boomgard et al. [1] the MEE nano-materials, (BiFeO3, BiTiO3-CoFe2O4, NiFe2O4-PZT) and their nanostructures became a significant role in research (Zheng et al. [2], Martinet al. [3], Wang et al. [4], Prashanthi et al. [5]). For this reason to the major potential of nanostructure for amplification of many applications, their mechanical behavior

Publisher: Peter the Great St. Petersburg Polytechnic University

should be investigated and well-identified before new designs can be proposed. The classical mechanic continuum theories demonstrate to predict the response of structures up to a minimum size sub which they fail to provide accurate predictions. The nonlocal theories add a size parameter in the modeling of the continuum. This paper studied models that developed according to the greatly used nonlocal elasticity theory (Eringen [6], Eringen [7], Eringen [8], Eringen [9], Eringen [10]). Timoshenko beam theory and nonlocal elasticity theory were investigated in their study. So based on an elastic medium, the stability response of SWCNT is described. Winkler and Pasternak parameter, an aspect ratio of the SWCNT, and nonlocal parameter was studied. Yang et al. [11] studied nonlinear free vibration of SWCNTs based on strains Eringen's nonlocal elasticity theory. Ehyaei and Akbarizadeh [12] illustrated the vibration analysis of micro composite thin beam based on modified couple stress theory.

A unified formulation for modeling the inhomogeneous nonlocal beams is developed by Ebrahimi and Barati [13]. Free vibration analysis of chiral double-walled carbon nanotube embedded in an elastic medium using nonlocal elasticity theory and Euler Bernoulli beam model was studied by Dihaj et al. [14]. Vibration and buckling of piezoelectric and piezomagnetic nanobeams based on third-order beam model are verified by Ebrahimi and Barati [16,17,18]. The vibration, buckling, and bending, free of Timoshenko nanobeams based on a meshless method were investigated by Roque et al. [19]. Embedded in the nonlocal component relevance of Eringen, a major of articles published searching to enlarge nonlocal beam models for nanostructures. Peddieson et al. [20] proposed the nonlocal Euler-Bernoulli and Timoshenko beam theory, accepted by many studies to verify bending (Civalek and Demir [21], Wang [22], Wang et al. [23]). During the years of research, the small size agents in SWCNTs were studied by Murmu and Pradhan [24]. Karami et al. [25] studied the wave propagation of functionally graded anisotropic nanoplates resting on the Winkler-Pasternak foundation. Ebrahimi and Rostami [26] analyzed the propagation of elastic waves in thermally affected embedded carbon-nanotube-reinforced composite beams via various shear deformation plate theories.

Free vibration analysis of a piezoelectric nanobeam using nonlocal elasticity theory is verified by Ali Hajnayeb and Foruzande [27]. Large amplitude forced vibration of the functionally graded nanocomposite plate with piezoelectric layers resting on the nonlinear elastic foundation was investigated by Yazdi [28]. Thermo-magneto-electro-elastic analysis of a functionally graded nanobeam integrated with functionally graded piezomagnetic layers was studied by Arefi and Zenkour [29]. Ebrahimi and Barati [30] investigated the wave propagation analysis of smart strain gradient piezo-magneto-elastic nonlocal beams. Arefi [31] checked the static analysis of laminated piezo-magnetic size-dependent curved beam based on modified couple stress theory. Jiang et al. [32] studied the analytical solutions to magneto-electro-elastic beams.

Furthermore, in recent years many researchers have presented the static and dynamic characteristics of beams and plates exposed to hygro-thermal environments because of the considerable effects of these environments on the structure's behavior. Gayen and Roy [33] presented an analytical method to determine the stress distributions in circular tapered laminated composite beams under hygro and thermal loadings. Kurtinaitiene et al. [34] investigated the effect of additives on the hydrothermal synthesis of manganese ferrite nanoparticles. Alzahrani et al. [35] investigated the size effects on the static behavior of nanoplates resting on elastic foundation subjected to hygro-thermal loadings. They extended the nonlocal constitutive relations of Eringen to contain the hygro-thermal effects. Also, Sobhy [36] studied the frequency response of simply-supported shear deformable orthotropic graphene sheets exposed to hygro-thermal loading.

Bending of Electro-mechanical sandwich nanoplate based on silica Aerogel foundation examined by Ghorbanpour et al. [37]. They described the influence of parameters on

nanostructure such as applied voltage, porosity index, foundation characteristics, parameter, plate aspect ratio, and thickness ratio on the bending response of sandwich nanoplate. Simsek et al. [38] presented three unknown shear and normal deformations nonlocal beam theories for the bending analysis of the problem. Ke et al. [39] studied the free vibration of size-dependent magneto-electro-elastic nanoplates based on the nonlocal theory. Selvamani and Ponnusamy [41-49] have proposed novel ideas in wave propagation analysis of different structures. Ramirez [50] investigated the discrete layer solution to free vibrations of functionally graded magneto-electro-elastic plates. Forooghi et al. [51] reported the thermal instability analysis of nanoscale FG porous plates embedded on the Kerr foundation coupled with fluid flow. Safarpour et al. [52] analyzed the theoretical and numerical solution for the bending and frequency response of graphene reinforced nanocomposite rectangular plates. Forooghi and Alibeigloo [53] studied the hygro-thermo-magnetically induced vibration of FG-CNTRC small-scale plate incorporating nonlocality and strain gradient size dependency. Vibrational frequencies of FG-GPLRC viscoelastic rectangular plate subjected to different temperature loadings based on higher-order shear deformation theory were proposed by Huang et al. [54].

This paper studies the bending of HMEE nanobeams bedded on a silica aerogel foundation based on nonlocal elasticity theory. Governing equations of a nonlocal nanobeam on Winkler-Pasternak substrate are derived via Hamilton's principle. Galerkin method is implemented to solve the governing equations. Effects of different factors such as nonlocal parameter, slenderness, moisture constant, critical temperature, applied voltage, magnet potential, and Young's modulus, and height of silica aerogel foundation on the deflection characteristics of a nanobeam are investigated.

2. Problem formulation

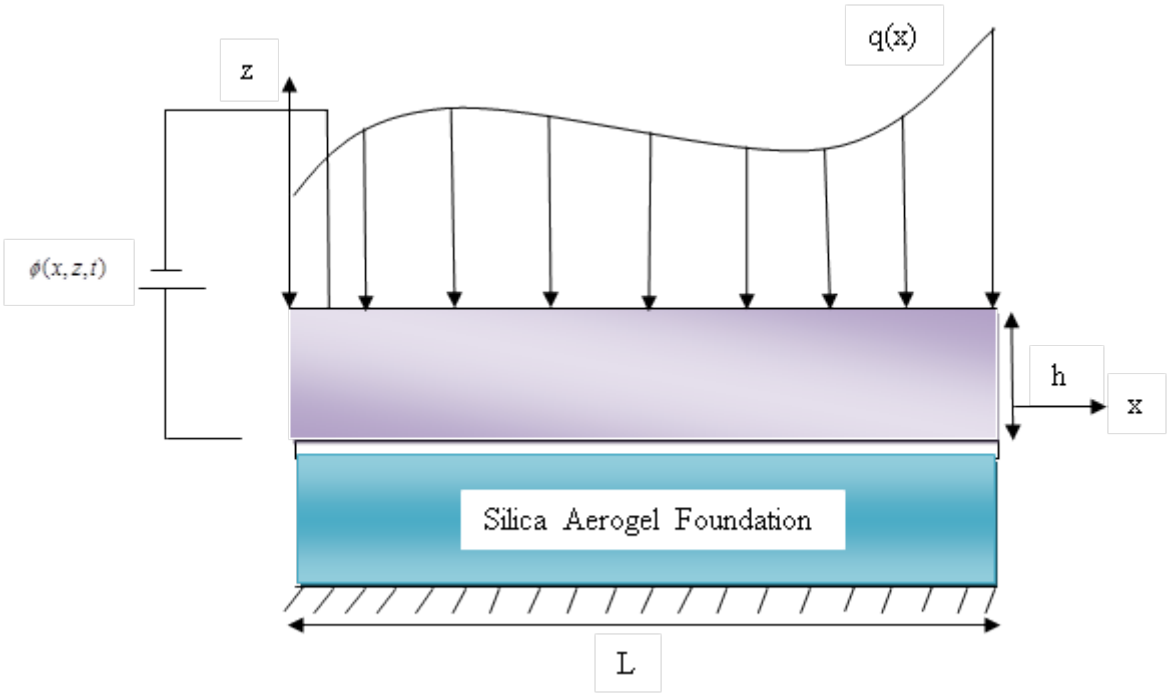

Fig. 1. Geometry of nanobeam resting on silica aerogel foundation

The component of displacement via refined shear deformable beam can be expressed by:

$$\boldsymbol{u_x(x,z) = u(x) - z\frac{\partial w_b}{\partial x} - f(z)\frac{\partial w_s}{\partial x}},\tag{1}$$

$$\boldsymbol{u_z(x,z) = w_b(x) + w_s(x)},\tag{2}$$

where u is axial mid-plane displacement and w_b, w_s denote the bending and shear components of transverse displacement, respectively. Also, $f(z)$ is the shape function representing the shear stress/strain distribution through the beam thickness which for the present study has a trigonometric essence, thus a shear correction factor is not required.

$$\boldsymbol{f(z)} = z + h_0 - tan[0.03(z + h_0)]. \tag{3}$$

Non-zero strains of the suggested beam model can be expressed as follows:

$$\varepsilon_{xx} = \frac{\partial u}{\partial x} - z\frac{\partial^2 w_b}{\partial x^2} - f(z)\frac{\partial^2 w_s}{\partial x^2}, \tag{4}$$

$$\gamma_{xz} = \mathrm{g}(z)\frac{\partial w_s}{\partial x}, \tag{5}$$

where $\mathrm{g}(z) = 1 - \partial f(z)/\partial z$.

According to Maxwell's equation, the relation between electric field (E_x, E_z) and electric potential (ϕ) and magnet field (Q_x, Q_z) and magnet potential (ψ), can be obtained as Ke et al. [39]:

$$E_x = -\phi_{,x} = \cos(\xi z)\frac{\partial \phi}{\partial x}\ , Q_x = -\psi_{,x} = \cos(\xi z)\frac{\partial \psi}{\partial x}, \tag{6}$$

$$E_z = -\phi_{,z} = \xi\sin(\xi z) - \frac{2v}{h}, Q_z = -\psi_{,z} = \xi\sin(\xi z) - \frac{2v}{h}, \tag{7}$$

where $\xi = \pi / h$. Also, V is the external electricity applied to the nanobeam.

Through extended Hamilton's principle, the governing equations can be derived as follows:

$$\int_0^t \delta(\Pi_S - \Pi_W)\mathrm{d}t = 0, \tag{8}$$

where Π_S is the total strain energy, Π_W is the work done by externally applied forces. The first variation of strain energy Π_S can be calculated as:

$$\delta\Pi_S = \int \sigma_{ij}\delta\varepsilon_{ij}dv = \int \sigma_x\delta\varepsilon_x + \sigma_{xz}\delta\gamma_{xz}. \tag{9}$$

Substituting equations (1) - (2) into equation (6) yields:

$$\begin{aligned}\Pi\mathrm{s} = {} & \int_0^a (N\frac{\partial \delta u}{\partial x} - M_b\frac{\partial^2 \delta w_b}{\partial x^2} - M_s\frac{\partial^2 \delta w_s}{\partial x^2} + Q\frac{\partial \delta w_s}{\partial x})dx + \\ & \int_0^a \int_{-h/2}^{h/2}\Big[-D_x\cos(\xi z)\frac{\partial \delta\phi}{\partial x} + D_z\xi\sin(\xi z)\,\delta\phi - \\ & B_x\cos(\xi z)\frac{\partial \delta\psi}{\partial x} + B_z\xi\sin(\xi z)\,\delta\varphi\psi\Big]\,dx\,dz,\end{aligned} \tag{10}$$

in which the forces and moments expressed in the above equation are defined as follows:

$$\begin{aligned}&(N, M_b, M_s) = \int_A (1, z, f)\sigma_i dA\ , i = (x, y, xy),\\ &Q_i = \int_A \mathrm{g}\sigma_i dA\ , i = (xz, yz)\ .\end{aligned} \tag{11}$$

The first variation of the work done by applied forces can be written in the form:

$$\delta\Pi_w = \int_0^l [(-N_x^0)\frac{\partial w}{\partial x}\frac{\partial \delta w}{\delta x} + (N^T + N^H)\frac{\partial (w_b + w_s)}{\partial x}\frac{\partial \delta (w_b + w_s)}{\delta x} - k_1\delta(w_b + w_s) + k_2\frac{\partial^2 (w_{b+}w_s)}{\partial x^2}]dx, \tag{12}$$

k_1, k_2 foundation parameters are as follows:

$$k_1 = \int_{-h/2-h_0}^{h/2-h_0} c_{11}\left(\frac{dx}{dz}\right)^2 dz,$$

$$k_2 = b\int_{-h/2-h_0}^{h/2-h_0} c_{44}x^2 dz.$$

Shape function of the foundation can be considered as:

$$x(z) = \frac{\sinh\gamma\left(1 - \dfrac{z}{H}\right)}{\sinh\gamma}.$$

In addition, γ is calculated by $\gamma^2 = H^2 \frac{c_{11}\int_{-\infty}^{\infty} \nabla w dx dy}{\int_{-\infty}^{\infty} w^2 dx dy}$,

where N^E, N^B electric, and magnet, loading respectively.

$N_x^0 = N^E + N^B$,

$N^E = -\int_{-h/2}^{h/2} e_{31} \frac{2V}{h} \mathrm{d}z,$ (13)

$N^B = -\int_{-h/2}^{h/2} e_{31} \frac{2\Omega}{h} \mathrm{d}z,$ (14)

where N^T, N^H are applied forces due to variation of temperature and moisture as

$N^T = \int_{-h/2}^{h/2} \mathrm{E(z)\alpha(z)\Delta T}\, dz,$ (15)

$N^H = \int_{-h/2}^{h/2} \mathrm{E(z)\beta(z)\Delta H}\, dz.$ (16)

The following Euler-Lagrange equations are obtained by inserting equations (10)-(12) in equation (8) when the coefficients of $\partial u, \partial w_b, \partial w_s, \emptyset, \psi$ are equal to zero:

$\frac{\partial N_x}{\partial x} = 0,$ (17)

$\frac{\partial^2 M_b}{\partial x^2} + (-N^E - N^B)\nabla^2(w_b + w_s) - (N^T + N^H)\frac{\partial^2 (w_{b+} w_s)}{\partial x^2} + k_1(w_b + w_s) - k_2\nabla^2(w_b + w_s) = 0,$ (18)

$\frac{\partial^2 M_s}{\partial x^2} - \frac{\partial Q}{\partial x} + (-N^E - N^B)\nabla^2(w_b + w_s) - (N^T + N^H)\frac{\partial^2 (w_{b+} w_s)}{\partial x^2} + k_1(w_b + w_s) - k_2\nabla^2(w_b + w_s) = 0,$ (19)

$\int_{-h/2}^{h/2} \left[\cos(\xi z)\frac{\partial D_x}{\partial x} + \xi \sin(\xi z)\, D_z\right] \mathrm{d}z = 0,$ (20)

$\int_{-h/2}^{h/2} \left[B_x \cos(\xi z)\frac{\partial \delta\psi}{\partial x} + B_z \xi \sin(\xi z)\, \delta\psi\right] \mathrm{d}z = 0.$ (21)

3. Nonlocal elasticity theory

The nonlocal theory can be extended for the piezo magnetic nanobeams as:

$\sigma_{ij-}(ea)^2\nabla^2\sigma_{ij} = \left[c_{ijkl}\varepsilon_{kl} - e_{mij}E_m - q_{nij}H_n - \alpha_{ij}T - \beta_{ij}H\right],$ (22)

$D_{ij-}(ea)^2\nabla^2 D_{ij} = [e_{ikl}\varepsilon_{kl} + k_{im}E_m + d_{in}H_n],$ (23)

$B_{i-}(ea)^2\nabla^2 B_i = [q_{ikl}\varepsilon_{kl} + d_{im}E_m + \varkappa_{in}H_n],$ (24)

$p_{i-}(ea)^2\nabla^2 p_i = \left[\varepsilon_0\chi_{ij}E_j + e_{ikl}\varepsilon_{kl}\right].$ (25)

Also, χ_{ij} is the relative dielectric susceptibility and f_{ijkl} is the flexoelectric coefficient. Also, $e_0 a$ is nonlocal parameter which is introduced to describe the size-dependency of nanostructures. ∇^2 is the Laplacian operator. The stress relations can be expressed by:

$(1 - \mu\nabla^2)\sigma_{xx} = (1 - \lambda^2\nabla^2)\left[C_{11}\varepsilon_{xx} - e_{31}E_z - q_{31}H_z - \alpha\Delta T - \beta\Delta H\right],$ (26)

$(1 - \mu\nabla^2)\sigma_{xz} = (1 - \lambda^2\nabla^2)[C_{55}\gamma_{xz} - e_{15}E_x - q_{15}H_x],$ (27)

$(1 - \mu\nabla^2)D_x = (1 - \lambda^2\nabla^2)[e_{15}\gamma_{xz} + k_{11}E_x + d_{11}H_x],$ (28)

$(1 - \mu\nabla^2)D_z = (1 - \lambda^2\nabla^2)[e_{31}\varepsilon_{xx} + k_{33}E_z + d_{33}H_z],$ (29)

$(1 - \mu\nabla^2)B_x = (1 - \lambda^2\nabla^2)[q_{15}\gamma_{xz} + d_{11}E_x + \varkappa_{11}H_x],$ (30)

$(1 - \mu\nabla^2)B_z = (1 - \lambda^2\nabla^2)[q_{31}\varepsilon_{xx} + d_{33}E_z + \varkappa_{33}H_x].$ (31)

Integrating equation (26-31) over the cross-section area of nanobeam provides the following nonlocal relations for a refined beam model as:

$$M_x = \int_{-h/2}^{h/2} \left(e_{31}\frac{2V}{h} + q_{31}\frac{2V}{h}\right) Z dz, \tag{32}$$

$$\int_{-h/2}^{h/2}(1-\mu\nabla^2)\{D_x\}\cos(\xi z)\,dz = F_{11}^e\left\{\frac{\partial\phi}{\partial x}\right\}, \tag{33}$$

$$\int_{-h/2}^{h/2}(1-\mu\nabla^2)\{B_x\}\cos(\xi z)\,dz = R_{11}^e\left\{\frac{\partial\psi}{\partial x}\right\}, \tag{34}$$

$$(1-\mu\nabla^2)\int_{-h/2}^{h/2}\xi\sin(\xi z)\,D_z dz = \left[A_{31}\left(\frac{\partial u}{\partial x}\right) - E_{31}\nabla^2 w\right], \tag{35}$$

$$(1-\mu\nabla^2)\int_{-h/2}^{h/2}\xi\sin(\xi z)\,B_z dz = \left[G_{31}\left(\frac{\partial u}{\partial x}\right) - Q_{31}\nabla^2 w\right], \tag{36}$$

in which:

$$\{A_{11}, B_{11}, B_{11}^s, D_{11}, D_{11}^s, H_{11}^s\} = \int_{-\frac{h}{2}}^{\frac{h}{2}} c11\,(1, z, f, z^2, fz, f^2)dz, \tag{37}$$

$$(A_{31}, E_{31}) = \int_{-h/2}^{h/2} e_{31}\xi\sin(\xi z)\{1, z, f\}_z dz, \tag{38}$$

$$(F_{11}, F_{33}) = \int_{-h/2}^{h/2}\{s_{11}\cos^2(\xi z), s_{33}\xi^2\sin^2(\xi z)\}dz, \tag{39}$$

$$(R_{11}, R_{33}) = \int_{-h/2}^{h/2}\{d_{11}\cos^2(\xi z), d_{33}\xi^2\sin^2(\xi z)\}dz, \tag{40}$$

$$(G_{31}, Q_{31}) = \int_{-h/2}^{h/2} q_{31}\xi\sin(\xi z)\{1, z\}_z dz, \tag{41}$$

$$(\varkappa_{11}, \varkappa_{33}) = \int_{-h/2}^{h/2}\{\varkappa_{11}\cos^2(\xi z), \varkappa_{33}\xi^2\sin^2(\xi z)\}dz. \tag{42}$$

The governing equations of nonlocal strain gradient nanoplate under electrical field in terms of the displacement can be derived by substituting equations (32) -(36), into equations (17) -(20) as follows:

$$\left[A_{11}\frac{\partial^2 u}{\partial x^2} - B_{11}\frac{\partial^3 w^b}{\partial x^3} - B_{11}^s\frac{\partial^3 w^s}{\partial x^3} + A_{31}\frac{\partial\phi}{\partial x} + G_{31}\frac{\partial\psi}{\partial x}\right] = \frac{\partial N_x}{\partial x}, \tag{43}$$

$$\begin{aligned}\left[[B_{11}\frac{\partial^3 u}{\partial x^3} - D_{11}\frac{\partial^4 w^b}{\partial x^4} - D_s^{11}\frac{\partial^4 w^s}{\partial x^4}] + E_{31}\frac{\partial^2\phi}{\partial x^2} + Q_{31}\frac{\partial^2\psi}{\partial x^2} + k_1(w_b + w_s) - k_2\nabla^2(w_b\right.\\ + w_s)] - \mu[(-N^E - N^B) + (N^T + N^H)\frac{\partial^2(w_{b+}w_s)}{\partial x^2}) + k_1(w_b + w_s)\\ \left. - k_2\nabla^2(w_b + w_s)]\right] = \frac{\partial^2 M_b}{\partial x^2},\end{aligned} \tag{44}$$

$$\begin{aligned}\left[\left[B_{11}^s\frac{\partial^3 u}{\partial x^3} - D_{11}^s\frac{\partial^4 w^b}{\partial x^4} - H_{11}^s\frac{\partial^4 w^s}{\partial x^4}\right] + F_{11}\frac{\partial^2\phi}{\partial x^2} + R_{11}\frac{\partial^2\psi}{\partial x^2} + k_1(w_b + w_s) - k_2\nabla^2(w_b\right.\\ + w_s)) - \mu[(-N^E - N^B) + (N^T + N^H)\frac{\partial^2(w_{b+}w_s)}{\partial x^2} + k_1(w_b + w_s)\\ \left. - k_2\nabla^2(w_b + w_s)]\right] = \frac{\partial^2 M_s}{\partial x^2} - \frac{\partial Q}{\partial x},\end{aligned} \tag{45}$$

$$[A_{31}\frac{\partial u}{\partial x} - E_{31}\frac{\partial^2 w^b}{\partial x^2} - Q_{31}\frac{\partial^2 w^s}{\partial x^2} + F_{11}\frac{\partial^2\phi}{\partial x^2} + R_{11}\frac{\partial^2\psi}{\partial x^2} - F_{33}\phi - R_{33}\psi = 0, \tag{46}$$

$$[A_{31}\frac{\partial u}{\partial x} - E_{31}\frac{\partial^2 w^b}{\partial x^2} - Q_{31}\frac{\partial^2 w^s}{\partial x^2} + F_{11}\frac{\partial^2\phi}{\partial x^2} + \varkappa_{11}\frac{\partial^2\psi}{\partial x^2} - F_{33}\phi - \varkappa_{33}\psi = 0. \tag{47}$$

4. Solution procedure

To satisfy the above-mentioned boundary conditions, the displacement quantities are presented in the following form:

$$u = \sum_{n=1}^{\infty} U_n\frac{\partial X_n(x)}{\partial x}e^{i\omega_n t}, \tag{48}$$

$$w_b = \sum_{n=1}^{\infty} W_{bn}X_n(x)e^{i\omega_n t}, \tag{49}$$

$$w_s = \sum_{n=1}^{\infty} W_{sn}X_n(x)e^{i\omega_n t}, \tag{50}$$

$\emptyset = \sum_{n=1}^{\infty} \emptyset_n X_n(x) e^{i\omega_n t}$, (51)

$\psi = \sum_{n=1}^{\infty} \psi_n X_n(x) e^{i\omega_n t}$, (52)

where (U_{mn} ,W_{bmn}, W_{zmn},$\emptyset, \psi$) are the unknown coefficients and for different boundary conditions ($\alpha = m\pi / a$, $\beta = n\pi / b$).

$$[K]\begin{Bmatrix} u_n \\ w_{bn} \\ w_{sn} \\ \phi \\ \psi \end{Bmatrix} = \begin{Bmatrix} 0 \\ Q_n(1+\mu\frac{n^2\pi^2}{L^2}) \\ Q_n\left(1+\mu\frac{n^2\pi^2}{L^2}\right) \\ 0 \\ 0 \end{Bmatrix}, \quad (53)$$

where [K], [F] are the stiffness, loading matrixes for nanobeam, respectively.

$k_{1,1} = A_{11}\alpha_1$, $K_{1,2} = B_{11}\alpha_2$, $K_{1,3} = B_{11}^s\alpha_2$, $K_{1,4} = A_{31}\alpha_3$, $K_{1,5} = G_{31}\alpha_3$ (54)

$K_{2,1} = B_{11}\alpha_{11}$, $k_{2,2} = -D_{11}\alpha_7 + k_1\alpha_5 - k_2\alpha_6 + \mu[(-N^E - N^B + (N^T + N^H) + k_2)\alpha_6 - k_1\alpha_5]$, $K_{2,3} = D_{11}^s\alpha_7 + k_1\alpha_5 - k_2\alpha_6 + \mu[(-N^E - N^B + (N^T + N^H) + k_2)\alpha_6 - k_1\alpha_5]$,

$k_{2,4} = E_{31}\alpha_6$, $k_{2,5} = Q_{31}\alpha_6$,

$K_{3,1} = B_{11}^s\alpha_{11}$, $K_{3,2} = -D_{11}^s\alpha_7 + \mu[(-N^E - N^B + (N^T + N^H) + k_2)\alpha_6 - k_1\alpha_5]$, $K_{3,3} = -H_{11}^s\alpha_7 + k_1\alpha_5 - k_2\alpha_6 + \mu[(-N^E - N^B + (N^T + N^H) + k_2)\alpha_6 - \left(k_1 + \frac{e_{31}}{2k_{33}}\right)f_{13}\alpha_5]$,

$k_{3,4} = F_{11}\alpha_6$, $k_{3,5} = R_{11}\alpha_6$,

$k_{4,1} = A_{31}\alpha_3$, $k_{4,2} = -E_{31}\alpha_6$, $k_{4,3} = -Q_{31}\alpha_6$, $k_{4,4} = F_{11}\alpha_6 - F_{33}\alpha_5$, $k_{4,5} = R_{11}\alpha_6 - R_{33}\alpha_5$,

$k_{5,1} = A_{31}\alpha_3$, $k_{5,2} = -E_{31}\alpha_6$, $5 = -Q_{31}\alpha_6$, $k_{4,4} = F_{11}\alpha_6 - F_{33}\alpha_5$, $k_{4,5} = \varkappa_{11}\alpha_6 - \varkappa_{33}\alpha_5$,

$F_{1,1} = N\alpha_3$,

$F_{2,2} = M_b(1-\mu\alpha_6)$,

$F_{3,3} = M_s(1-\mu\alpha_6) - Q(1-\mu\alpha_3)$,

in which (Table 1):

$\alpha_1 = \int_0^a X'(x)X''(x)\,dx$, $\alpha_2 = \int_0^a X(x)X'''(x)\,dx$, $\alpha_7 = \int_0^a X(x)X''''(x)\,dx$, (55)

$\alpha_5 = \int_0^a X(x)\,X(x)dx$, $\alpha_3 = \int_0^a X(x)\,X'(x)dx$, $\alpha_{11} = \int_0^a X'(x)X'''(x)\,dx$,

$\alpha_6 = \int_0^a X(x)X''(x)\,dx$.

The uniform load is supposed that lead to bending and is expressed by the following form:

$q_{dynamics} = \sum_{n=1}^{\infty} Q_n \sin[\frac{n\pi}{L}x]\sin\omega t$, (56)

$Q_n = \frac{2}{L}\int_{x_0-c}^{x_0+c} \sin[\frac{n\pi}{L}x]q_x dx$, (57)

in which Q_n are the Fourier coefficients and $q(x) = q_0$ is the uniform load density and x_0 is the centroid coordinate. Also, in the case of concentrated point load the following expression for the harmonic load intensity can be written:

$q(x) = p\delta(x - x_0)\sin\omega t$, (58)

$Q_n = \frac{2p}{L}\sin\left[\frac{n\pi}{L}x_0\right]$, (59)

in which δ is the Dirac delta.

Table 1. The admissible functions $X_m(x)$ Sobhy [36]

	Boundary conditions	The functions X_m
	At x=0, a	$X_m(x)$
SS	$X_m(0) = X_m''(0) = 0$	$Sin(\alpha x)$
	$X_m(a) = X_m''(a) = 0$	

5. Numerical results and discussions

The bending of hygro magneto thermo piezoelectric nanobeam is analyzed in this section. The material properties are shown in Table 2 (Ramirez et al. [50]). The validity of the present study is proved by the means of comparing the bending of this model with those of Arefi and Zenkour [29]. Arefi and Zenkour [29] for various nonlocal parameters are presented in Table 3.

Table 2. Material properties of $BiTiO_3$-$CoFe_2O_4$ composite materials

Properties	$BiTiO_3$-$CoFe_2O_4$
Elastic (GPa)	c_{11} = 226, c_{12} = 125, c_{13} = 124, c_{33} = 216, c_{44} = 44.2, c_{66} = 50.5
Piezoelectric/(C ⋅ m^{-2})	e_{31} = −2.2, e_{33} = 9.3, e_{15} = 5.8
Dielectric/(10^{-9}C ⋅ V^{-1} ⋅ m^{-1})	k_{11} = 5.64, k_{33} = 6.35
Piezomagnetic/(N ⋅ A^{-1} ⋅ m−1)	q_{15} = 275, q_{31} = 290.1, q_{33} = 349.9
Magnetoelectric/(10^{-12}Ns ⋅ V^{-1} ⋅ C^{-1})	s_{11} = 5.367, s_{33} = 2 737.5
Magnetic ($10^{-6}\ Ns^2\ c^{-2}/2$)	$\varkappa_{11}$ = -297, $\varkappa_{33}$ = 83.5
Mass density(10^3Kg/m^3)	ρ=5.55
Hygrothermal(/K)	$\alpha_{eff} = 1.6\times10^{-6}$ $\beta_{eff} = 26\times10^{-4}$

Table 3. Comparison of dimensionless deflections of nanobeam for electric voltage and magnet potential

L/h	μ(nm^2)	$\psi = 0.001$		L/h	μ(nm^2)	$\phi = 0.001$	
		Arefi and Zenkour [29]	present			Arefi and Zenkour [29]	Present
10	1	3.68	3.5781	10	0	3.68	3.59892
	2	3.71	3.6482		1	1.3333	3.66921
	3	3.77	3.7302		2	1.3645	3.74018
	4	3.84	3.79011		3	1.3958	3.80234
	5	3.94	3.8952		4	1.4270	3.92011

The role of various parameters like magnetic potential (Ω), electric voltage (V), moisture constant (ΔH), and nonlocal parameter (μ) on the non-dimensional frequencies of the simply supported higher-order magneto-electro-elastic nanobeams at L/h =20 and L/h =30 are exposed in Tables 4 and Table 5. Here, it is noticeable that with the rise of nonlocal parameters the natural frequencies of hygro magneto-electro-elastic nanobeam reduces for all magnetic potentials and external voltages due to the fact that the existence of nonlocality weakens the beam. Also, it is referred that when the moisture constant arose the

non-dimensional frequencies of hygro magneto-electro-elastic nanobeam decrease, especially for lower moisture constant. Moreover, it is concluded that negative values of magnetic potential and external electric voltage produce lower/higher frequencies compared to those of positive ones, respectively.

Table 4. Variation of the third dimensionless frequency of FG nanobeam for the various nonlocal parameters, magnetic potentials, and electric voltages (L/h =30)

μ		Ω=-0.05			Ω=0			Ω=+0.05		
		ΔH	ΔH =1	ΔH =5	ΔH	ΔH =1	ΔH =5	ΔH=0.	ΔH =1	ΔH =5
0	V=-	78.077	71.962	68.082	78.967	72.525	68.275	79.848	73.084	68.467
	V=0	77.941	71.532	67.345	78.833	72.099	67.540	79.715	72.661	67.735
	V=+	77.804	71.100	66.600	78.698	71.670	66.797	79.582	72.235	66.994
1	V=-	56.325	52.280	49.892	57.553	53.053	50.156	58.756	53.814	50.417
	V=0	56.136	51.687	48.882	57.369	52.468	49.151	58.575	53.238	49.418
	V=+	55.947	51.087	47.850	57.184	51.877	48.125	58.394	52.655	48.397
2	V=-	46.039	43.041	41.429	47.534	43.976	41.746	48.983	44.891	42.060
	V=0	45.808	42.318	40.207	47.310	43.269	40.533	48.766	44.199	40.856
	V=+	45.576	41.583	38.946	47.085	42.550	39.282	48.548	43.496	39.616
3	V=-	39.712	37.400	36.307	41.436	38.472	36.668	43.091	39.515	37.025
	V=0	39.444	36.566	34.905	41.179	37.662	35.280	42.844	38.727	35.651
	V=+	39.174	35.712	33.445	40.921	36.834	33.836	42.596	37.922	34.223

Table 5. Dispersion of dimensionless frequency of nanobeam for the various nonlocal parameters, magnetic potentials, and electric voltages (L/h =20)

μ		Ω=-0.05			Ω=0			Ω=+0.05		
		ΔH	ΔH =1	ΔH =5	ΔH	ΔH =1	ΔH =5	ΔH	ΔH =1	ΔH =5
0	V=-	35.608	32.956	31.424	36.477	33.504	31.611	37.325	34.044	31.797
	V=0	35.474	32.534	30.705	36.346	33.089	30.896	37.198	33.635	31.087
	V=+	35.340	32.107	29.968	36.215	32.669	30.164	37.070	33.222	30.359
1	V=-	29.900	27.860	26.782	30.929	28.506	27.002	31.926	29.139	27.219
	V=0	29.741	27.360	25.934	30.775	28.018	26.161	31.777	28.661	26.385
	V=+	29.581	26.850	25.058	30.621	27.520	25.292	31.627	28.174	25.524
2	V=-	26.174	24.556	23.798	27.344	25.287	24.044	28.466	25.998	24.288
	V=0	25.992	23.987	22.839	27.170	24.735	23.096	28.299	25.461	23.350
	V=+	25.808	23.404	21.838	26.994	24.170	22.107	28.130	24.912	22.372
3	V=-	23.487	22.191	21.678	24.784	22.997	21.948	26.017	23.776	22.215
	V=0	23.284	21.559	20.621	24.592	22.388	20.905	25.834	23.188	21.185
	V=+	23.079	20.909	19.507	24.398	21.763	19.806	25.650	22.584	20.102

The length of nanobeam is considered to be L = 10 nm. Also, the dimensionless deflection is adopted as

$$W = 100\frac{C_{11}I}{q_0L^4}. \quad (60)$$

Figures 2 and 3 investigated for the effect of nonlocal parameters on a dimensionless deflection through various magnetic potential, it is found that increasing the value of the nonlocal parameters caused the increase in dimensionless deflection but positive electric voltage leads to a reduction in deflection and negative potential rise the dimensionless deflection. We understand from this subject that magnetic potential has a significant role under dimensionless deflection and also dimensionless deflection null effect during zero electric voltage. The effect of humidity is observed in Fig. 3 through the rise in dimensionless deflection.

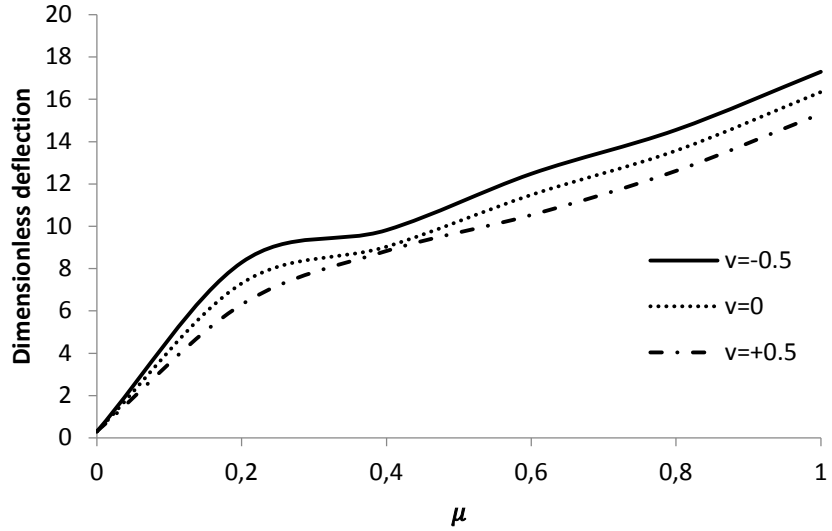

Fig. 2. Effect of nonlocal parameters on dimensionless deflection via $\Omega = 0.5$ (L/*h*=10, $K_w = K_p$=20, ΔH=1.5)

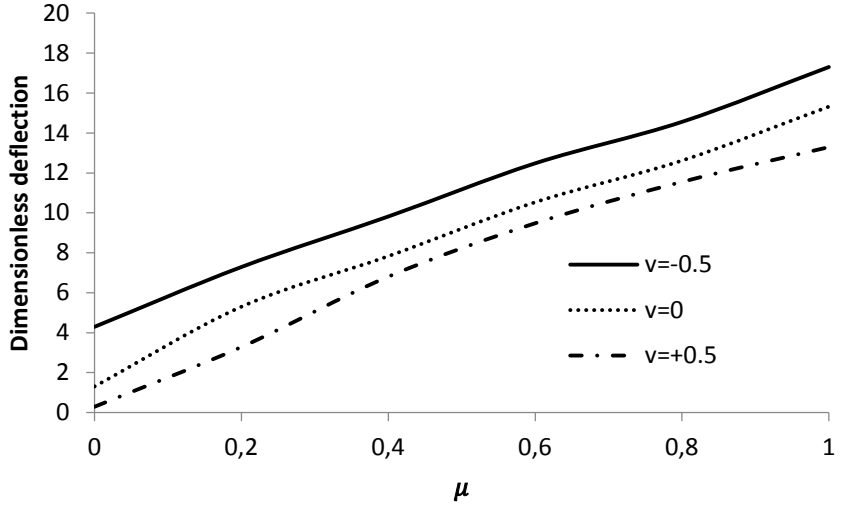

Fig. 3. Effect of nonlocal parameters on dimensionless deflection via $\Omega = 1.5$ (L/*h*=10, $K_w = K_p$=20, ΔH=1.5)

Dimensionless deflection of the nanobeam with respect to slenderness ratio through various electric voltages are presented in Figs. 4 and 5. It is found that the external electric voltage caused that softening deflection of nanobeam for positive values and external voltage for negative values of nanobeam demonstrated a hardening effect. From this, the axial tensile and compressive forces are exposed in the nanobeams via the constructed positive and negative voltages, respectively. In addition, it is lightly observed that the dimensionless

deflection is approximately independent of the slenderness ratio for zero electric voltages ($V=0$**)**. The increase in magnetic potential hardens the deflection.

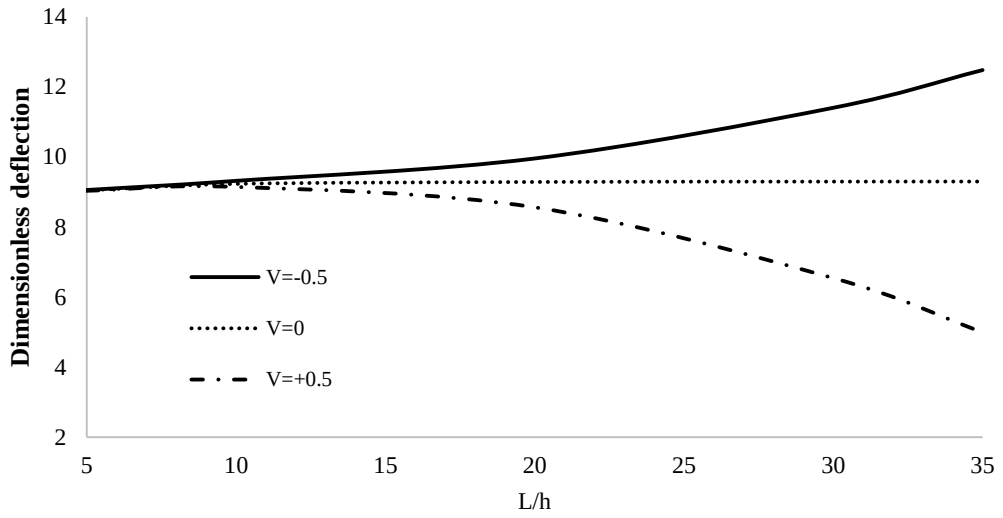

Fig. 4. Effect of slenderness ratio on dimensionless deflection via $\Omega = 0.5$ (L/*h*=10, K_w= K_p=20, ΔH=1.5)

.

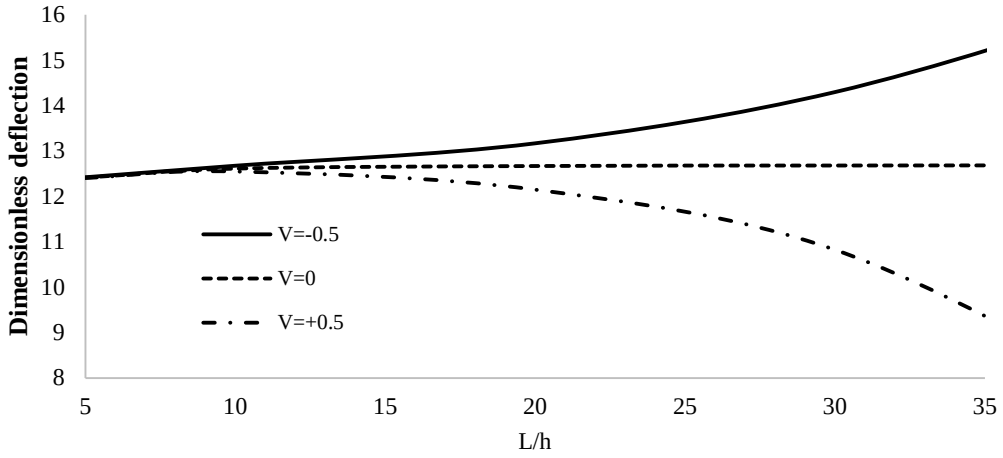

Fig. 5. Effect of slenderness ratio on dimensionless deflection via $\Omega = 1.5$ (L/*h*=10, K_w= K_p=20, ΔH=1.5)

Figures 6 and 7 are demonstrated for the variation of dimensionless deflection of nanobeam with the moisture constant via various magnetic potentials. In this example, the rise in moisture constants improves the value of deflection. Also, it is referred that the positive voltage values stiffen the deflection more than the negative voltage. This result also indicates that the effect of moisture weakens the nanobeam. The obtained results of these figures indicate that the maximum deflection increases with increasing the magnetic potential of the nanobeam.

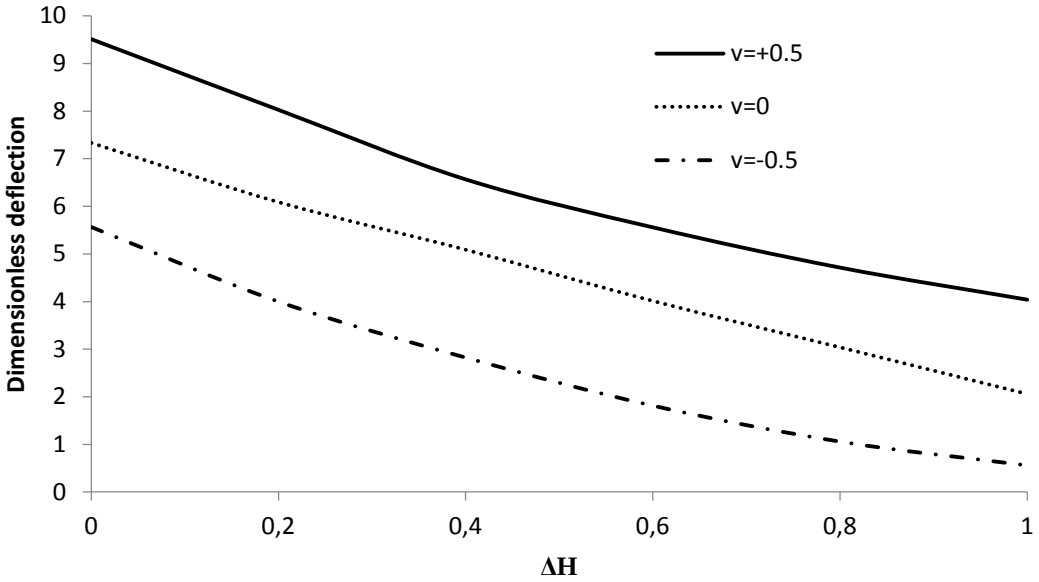

Fig. 6. Effect of moisture constant versus dimensionless deflection via $\Omega = 0.5$ (L/h=10, K_p =K_w=20)

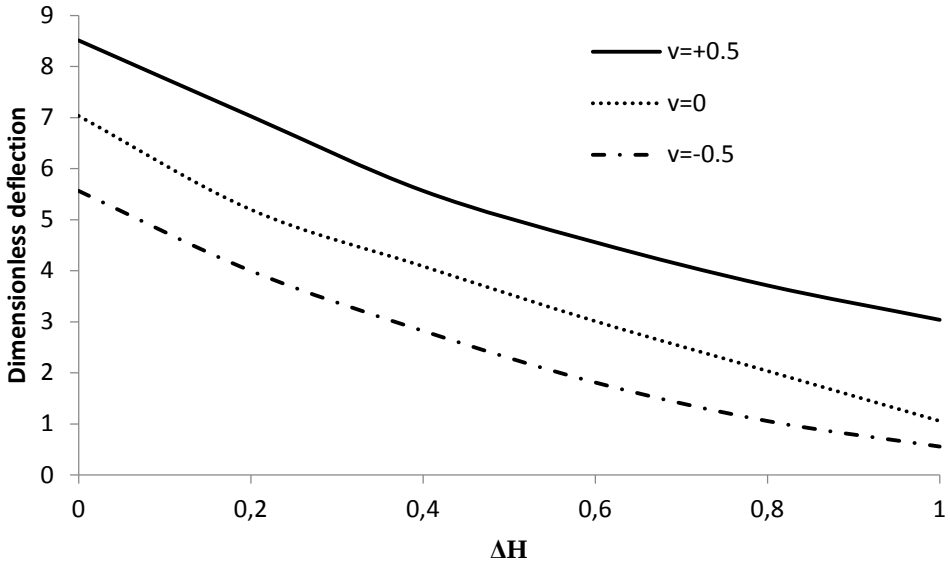

Fig. 7. Effect of moisture constant versus dimensionless deflection via $\Omega = 1.5$ (L/h=10, K_p =K_w=20)

Figures 8-9 expresses the effect of critical temperature on the dimensionless deflection via moisture coefficient rise with different electric voltage values. It can be noticed that the rise in critical temperature drives to reduce the dimensionless deflection. Also, the moisture coefficient rise expose the less amount of magnitude rise in dimensionless deflection while an increase in temperature values. The results expose the truth that the moisture coefficient variations soften the variant values via critical temperature.

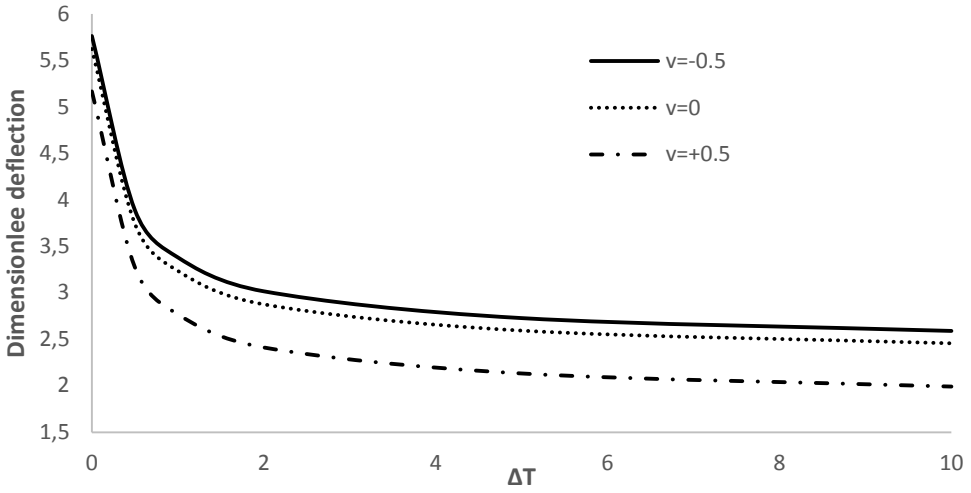

Fig. 8. Effect of critical temperature versus dimensionless deflection via ΔH=0.5 (*L/h*=10, K_p =K_w=20, $\Omega = 0$)

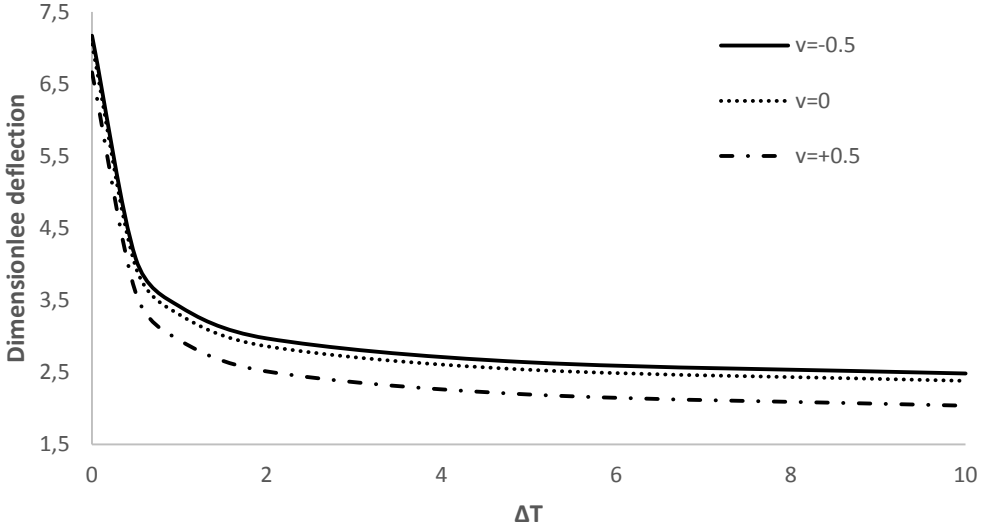

Fig. 9. Effect of critical temperature versus dimensionless deflection via ΔH=1.5 (*L/h*=10, K_p =K_w=20, $\Omega = 0$)

The variations of the dimensionless deflection of nanobeams versus Young's modulus of silica aerogel foundation for various electric voltages are shown in Figs. 10 and 11, respectively. It is found from this figure that regardless of the sign and magnitude of electric voltage, the dimensionless deflection decreases with the increase of Young's modulus of silica aerogel foundation, so the stiffness weakens of the nanobeam. It must be mentioned that the rise in magnetic potential provides higher deflection.

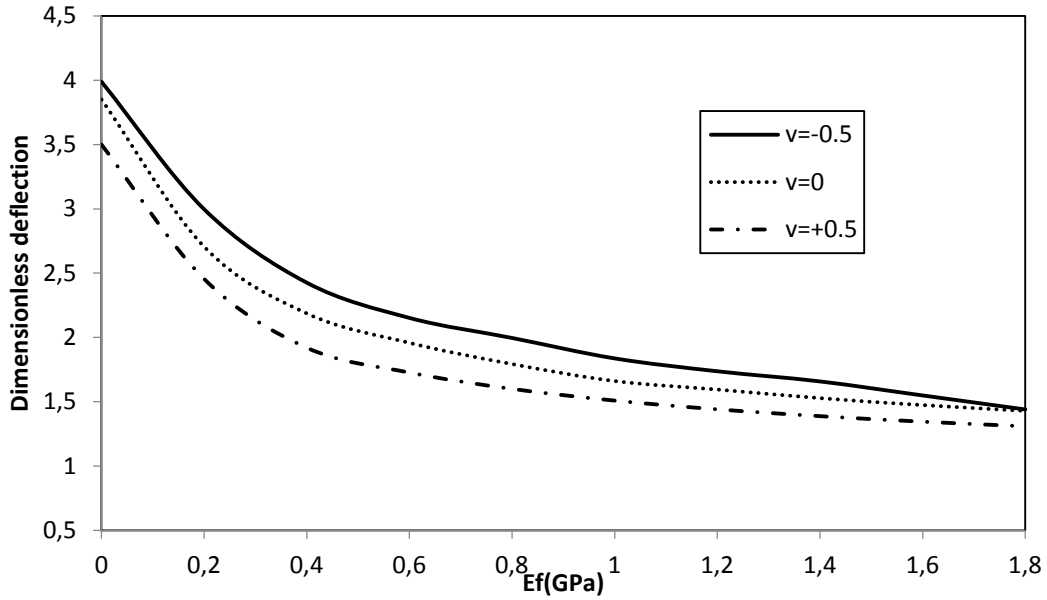

Fig. 10. Effect of Young's modulus of silica aerogel foundation versus dimensionless deflection $\Omega = 0.5$ (L/h=10, $\mu = 2, \Delta H = 1.5$)

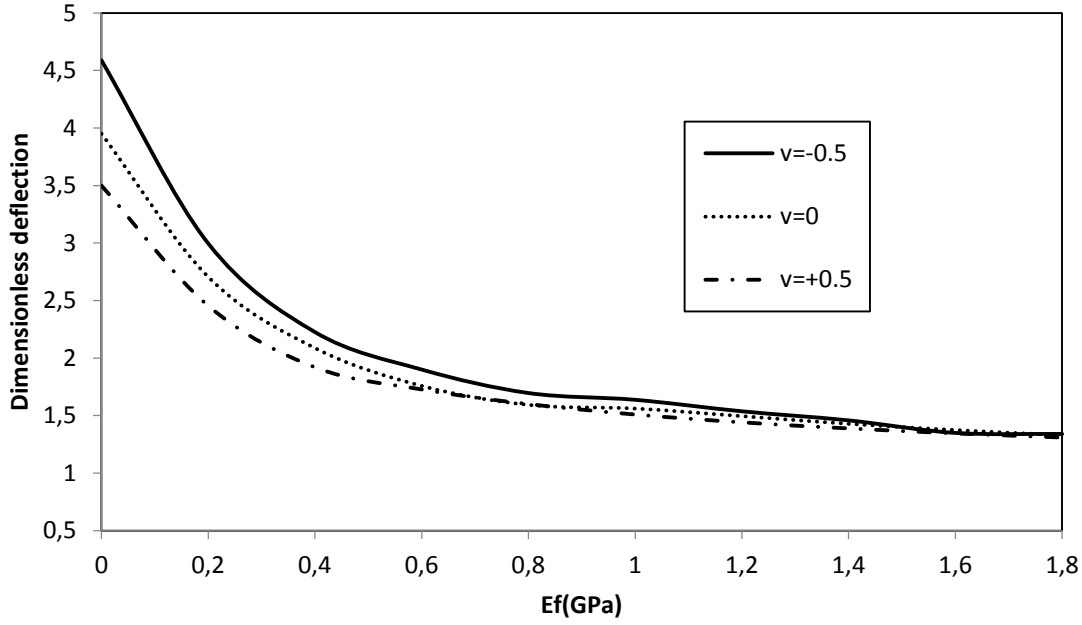

Fig. 11. Effect of Young's modulus of silica aerogel foundation versus dimensionless deflection $\Omega = 1.5$ (L/h=10, $\mu = 2, \Delta H = 1.5$)

The effect of height of the silica aerogel foundation on dimensionless deflection is recorded in Figs. 12 and 13. By raising the height of the silica aerogel foundation the dimensionless deflection is amplified for different applied electric voltages. Again the effect of higher values of magnetic potential is pronounced.

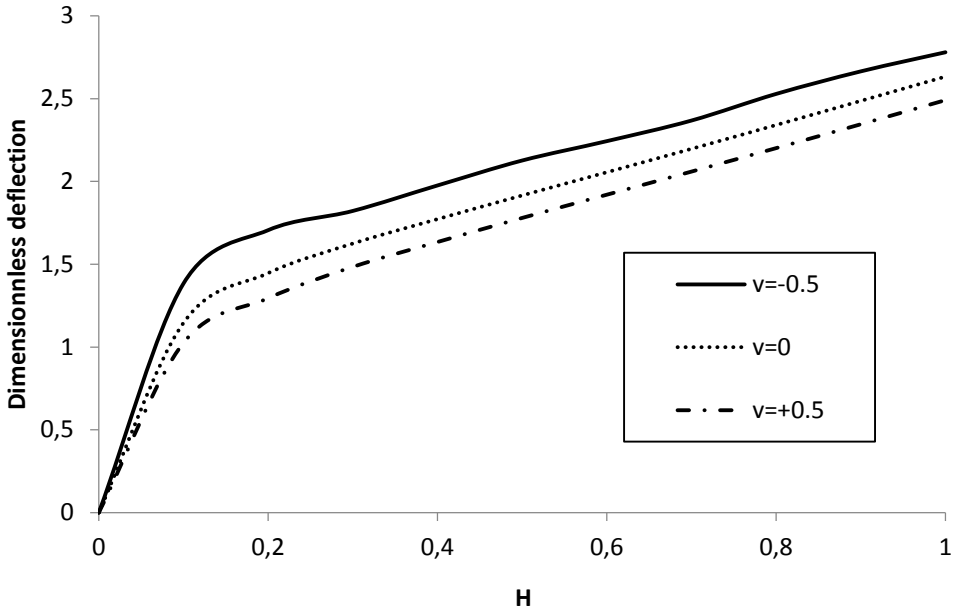

Fig. 12. Effect of Young's modulus of silica aerogel foundation versus dimensionless deflection $\Omega = 1.5$ (L/h=10, $\mu = 2, \Delta H = 1.5$)

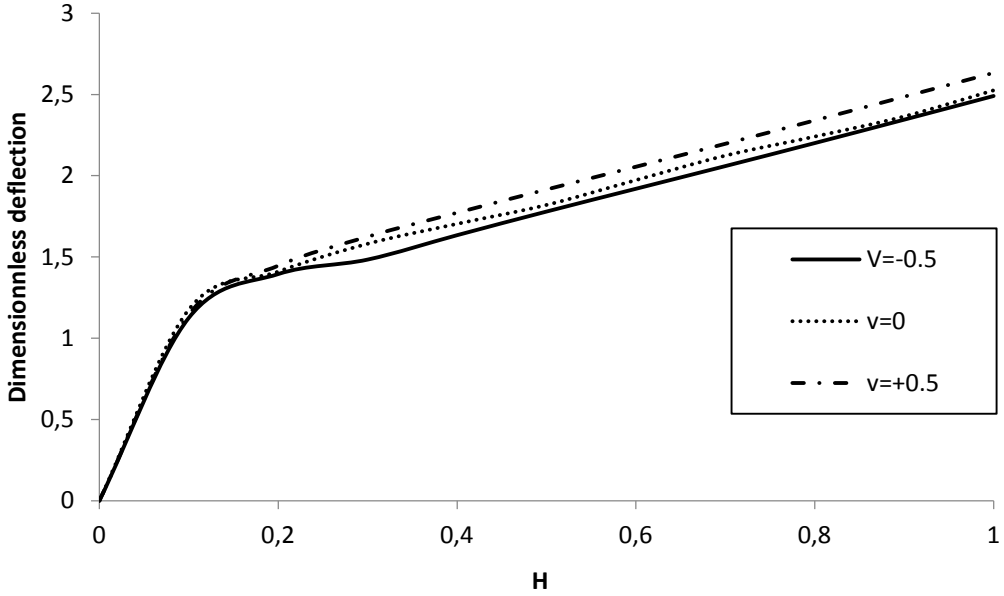

Fig. 13. Effect of Young's modulus of silica aerogel foundation versus dimensionless deflection $\Omega = 1.5$ (L/h=10, $\mu = 2, \Delta H = 1.5$)

6. Conclusions

External electric voltages on the deflection of Hygro-magneto-electro-elastic (HMEE) nanobeams embedded on silica aerogel foundation are studied in this article. The governing equations of nonlocal nanobeams based on higher-order refined beam theory are obtained using Hamilton's principle and solved by analytical solution. A parametric study is presented to observe the effect of the nonlocal parameter, slenderness, moisture constant, critical temperature, and the foundation constants on the deflection characteristics of nanobeam via different applied electric voltages. Some of the bolded highlights of this research are as follows.

- The dimensionless deflection can be amplified using the higher nonlocal parameters.
- The maximum dynamic response can be arrived at by choosing higher magnetic intensity.
- The system's dimensionless deflection can be gradually amplified when the electric voltage is negative.
- The moisture values soften the dimensionless deflection in the presence of magnetic potential.
- The dimensionless deflection may be weakened by bigger values of critical temperature in a humid environment.
- The higher density of foundation (Young's modulus of silica aerogel) reduces the stiffness of the nanobeam. On the other hand, the increase in height of th foundation refers to an amplified deflection
- The compressive and tensile nature is proven in the deflection of nanobeams via positive and negative voltage generation.

References

1. Van den Boomgard J, Terrell DR, Born RAJ. An in situ grown eutectic magnetoelectric composite material. *Journal of Materials Science*. 1974;9: 1705-1709.
2. Zheng H, Wang J, Lofland SE. Multiferroic BaTiO3-CoFe2O4 nanostructures. *Science*. 2004;303(5658): 661-663.
3. Martin LW, Crane SP, Chu YH. Multiferroics and magnetoelectrics: Thin films and nanostructures. *Journal of Condensed Matter Physics*. 2008;20(43): 434220.
4. Wang Y, Hu JM. Lin YH. Multiferroic magnetoelectric composite nanostructures. *NPG Asia Materials*. 2010;2: 61-68.
5. Prashanthi K, Shaibani PM, Sohrabi A. (2012), Nanoscale magnetoelectric coupling in multiferroic BiFeO3 nanowires. *Physica Status Solidi - Rapid Research Letetrs*. 2012;6(6): 244-246.
6. Eringen, A. Nonlocal polar elastic continua. *International Journal of Engineering Science*. 1968;10(1): 1-16.
7. Eringen A. Nonlocal micropolar field theory. In: *Continuum Physics.* Eringen A.C. (Ed.) New York: Academic Press; 1976. p.106.
8. Eringen A. *Nonlocal Continuum Field Theories*. New York: Springer; 2002.
9. Eringen A. Nonlocal continuum mechanics based on distributions. *International Journal of Engineering Science*. 2006;44(3): 141-147.
10. Eringen A, Edelen D. On nonlocal elasticity. *International Journal of Engineering Science*. 1972;10(3): 233-248.
11. Yang J, Ke LL, Kitipornchai S. Nonlinear free vibration of single-walled carbon nanotubes using nonlocal Timoshenko beam theory. *Physica E: Low-Dimensional Systems and Nanostructures*. 2010;42(5): 1727-1735.
12. Ehyaei J. Akbarizadeh MR. Vibration-analysis of micro composite thin beam based on modified couple stress. *Structural Engineering and Mechanics*. 2017;64(4): 793-802.
13. Ebrahimi F, Barati MR. Wave propagation analysis of smart strain gradient piezo-magneto-elastic nonlocal beams. *Structural Engineering and Mechanics*. 2018;66(2): 237-248.
14. Dihaj A, Zidour M, Meradjah M, Rakrak K, Heireche H, Chemi A. Free vibration analysis of chiral double-walled carbon nanotube embedded in an elastic medium using non-local elasticity theory and Euler Bernoulli beam model. *Structural Engineering and Mechanics*. 2018;65(3): 335-342.
15. Ebrahimi F, Barati MR. Dynamic modeling of a thermo–piezo-electrically actuated nanosize beam subjected to a magnetic field. *Applied Physics Research*. 2016;122(4): 1-18.

16. Ebrahimi F, Barati MR. Electromechanical buckling behavior of smart piezoelectrically actuated higher-order size-dependent graded nanoscale beams in thermal environment. *International Journal of Smart and Nano Materials*. 2016;7(2): 69-70.
17. Ebrahimi F, Barati MR. An exact solution for buckling analysis of embedded piezoelectro-magnetically actuated nanoscale beams. *Advances in Nano Research*. 2016c;4(2): 65-84.
18. Ebrahimi F, Barati MR. Vibration analysis of smart piezoelectrically actuated nanobeams subjected to magneto-electrical field in thermal environment. *Journal of Vibration and Control*. 2018;24(3): 549-564.
19. Roque CMC, Ferreira AJM, Reddy JN. Analysis of Timoshenko nanobeams with a nonlocal formulation and meshless method. *International Journal of Engineering Science*. 2011;49(9): 976-984.
20. Peddieson J, Buchanan GR, McNitt RP. Application of nonlocal continuum models to nanotechnology. *International Journal of Engineering Science*. 2003;41(3-5): 305-312.
21. Civalek O, Demir C. Bending analysis of microtubules using nonlocal Euler–Bernoulli beam theory. *Applied Mathematical Modelling*. 2011;35(5): 2053-2067.
22. Wang Q. Wave propagation in carbon nanotubes via nonlocal continuum mechanics. *International Journal of Applied Physics*. 2005;98(12): 124-301.
23. Wang CM, Kitipornchai S, Lim CW, Eisenberger M. Beam bending solutions based on nonlocal Timoshenko beam theory. *Journal of Engineering Mechanics*. 2008;134(6): 475-481.
24. Murmu T, Pradhan SC. Buckling analysis of a single-walled carbon nanotube embedded in an elastic medium based on nonlocal elasticity and Timoshenko beam theory and using DQM. *Physica E: Low-Dimensional Systems and Nanostructures*. 2009;41(7): 1232-1239.
25. Karami B, Janghorban M, Tounsi A. Effects of triaxial magnetic field on the anisotropic nanoplates. Steel. *Composite Structures*. 2017;25(3): 361-374.
26. Ebrahimi F, Rostami P. Propagation of elastic waves in thermally affected embedded carbon-nanotube-reinforced composite beams via various shear deformation plate theories. *Structural Engineering and Mechanics*. 2018;66: 495-504.
27. Ali Hajnayeb AK, Foruzande H. Free vibration analysis of a piezoelectric nanobeam using nonlocal elasticity theory. *Structural Engineering and Mechanics*. 2017;61(5): 617-624.
28. Yazdi AA. Large amplitude forced vibration of functionally graded nano-composite plate with piezoelectric layers resting on nonlinear elastic foundation. *Structural Engineering and Mechanics*. 2018; 68(2): 203-213.
29. Arefi M, Zenkour AM. A simplified shear and normal deformations nonlocal theory for bending of functionally graded piezomagnetic sandwich nanobeams in magneto-thermo-electric environment. *Journal of Sandwich Structures and Materials*. 2016;18(5): 624-651.
30. Ebrahimi F, Barati MR. Buckling analysis of nonlocal third-order shear deformable functionally graded piezoelectric nanobeams embedded in elastic medium. *Journal of the Brazilian Society of Mechanical Sciences and Engineering*. 2016;39: 937-952.
31. Arefi M. Static analysis of laminated piezo-magnetic size-dependent curved beam based on modified couple stress theory. *Structural Engineering and Mechanics*. 2019;69: 145-153.
32. Jiang A, Haojiang D. Analytical solutions to magneto-electro-elastic beams. *Structural Engineering and Mechanics*. 2004;18(2): 195-209.
33. Gayen D, Roy T. Hygro-thermal effects on stress analysis of tapered laminated composite beam. *International Journal of Composite Materials*. 2013;3(3): 46-55.
34. Kurtinaitiene M, Mazeika K, Ramanavicius S, Pakstas V, Jagminas A. Effect of additives on the hydrothermal synthesis of manganese ferrite nanoparticles. *Advances in Nano Research*. 2016;4(1): 1-14.

35. Alzahrani EO, Zenkour AM, Sobhy M. Small scale effect on hygro-thermo-mechanical bending of nanoplates embedded in an elastic medium. *Composite Structures*. 2013;105: 163-172.
36. Sobhy M. Buckling and free vibration of exponentially graded sandwich plates resting on elastic foundations under various boundary conditions. *Composite Structures*. 2013;99: 76-87.
37. Ghorbanpour Arani A, Zamani MH. Investigation of electric field effect on size-dependent bending analysis of functionally graded porous shear and normal deformable sandwich nanoplate on silica Aerogel foundation. *Journal of Sandwich Structures and Materials*. 2017;1099636217721405.
38. Şimşek M, Yurtcu HH. Analytical solutions for bending and buckling of functionally graded nanobeams based on the nonlocal Timoshenko beam theory. *Composite Structures*. 2013;97: 378-386.
39. Ke LL, Wang YS, Yang J, Kitipornchai S. Free vibration of size-dependent magneto-electro-elastic nano plates based on the nonlocal theory. *Acta Mechanica Solida Sinica*. 2014;30(4): 516-525.
40. Selvamani R, Ponnusamy P. Damping of generalized thermoelastic waves in a homogeneous isotropic plate. *Materials Physics and Mechanics*. 2012;14(1): 64-73.
41. Selvamani R.Influence of thermo-piezoelectric field in a circular bar subjected to thermal loading due to laser pulse. *Materials Physics and Mechanics*. 2016;27(1): 1-8.
42. Selvamani R. Free vibration analysis of rotating piezoelectric bar of circular cross section immersed in fluid. *Materials Physics and Mechanics*. 2015;24(1): 24-34.
43. Selvamani R. Dynamic response of a heat conducting solid bar of polygonal cross sections subjected to moving heat source. *Materials Physics and Mechanics*. 2014;21(2): 177-193.
44. SelvamaniR, Ponnusamy P. Elasto Dynamic wave propagation in a transversely isotropic piezoelectric circular plate immersed in Fluid. *Materials Physics and Mechanics.* 2013;17(2): 164-177.
45. Selvamani R, Ponnusamy P. Effect of rotation in an axisymmetric vibration of a transversely isotropic solid bar immersed in an inviscid fluid. *Material Physics and Mechanics*. 2012;15(2): 97-106.
46. Selvamani R, Sujitha G. Effect of non-homogeneity in a magneto electro elastic plate of polygonal cross-sections. *Materials Physics and Mechanics*. 2018;40(1): 84-103.
47. Selvamani R, Flexural wave motion in a heat conducting doubly connected thermo-elastic plate of polygonal cross-sections. *Materials Physics and Mechanics*. 2014;19(1): 51-67
48. Selvamani R, Ponnusamy P. Generalized thermoelastic waves in a rotating ring shaped circular plate immersed in an inviscid fluid. *Materials Physics and Mechanics*. 2013;18(1): 77-92.
49. Selvamani R, Ponnusamy P. Extensional Waves in a Transversely Isotropic Solid Bar Immersed in an Inviscid Fluid Calculated Using Chebyshev Polynomials. *Materials Physics and Mechanics*. 2013;16(1): 82-91.
50. Ramirez F, Heyliger PR, Pan E. Discrete layer solution to free vibrations of functionally graded magneto-electro-elastic plates. *Mechanics of Advanced Materials and Structures*. 2006;13(3): 249-266.
51. Forooghi A, Rezaey S, Haghighi SM, Zenkour AM. Thermal instability analysis of nanoscale FG porous plates embedded on Kerr foundation coupled with fluid flow. *Engineering with Computers*. 2021. Available from: https://doi.org/10.1007/s00366-021-01426-3.
52. Safarpour M, Forooghi A, Dimitri R, Tornabene F. Theoretical and Numerical Solution for the Bending and Frequency Response of Graphene Reinforced Nanocomposite Rectangular Plates. *Applied Sciences*. 2021;11(14): 6331.

53. Forooghi A, Alibeigloo A. Hygro-thermo-magnetically induced vibration of FG-CNTRC small-scale plate incorporating nonlocality and strain gradient size dependency. *Waves in Random and Complex Media*. 2022. Available from: https://doi.org/10.1080/17455030.2022.2037784.
54. Huang W, Ren J, Forooghi A. Vibrational frequencies of FG-GPLRC viscoelastic rectangular plate subjected to different temperature loadings based on higher-order shear deformation theory and utilizing GDQ procedure. *Mechanics Based Design of Structures and Machines*. 2021. Available from: https://doi.org/10.1080/15397734.2021.1878041.

THE AUTHORS

Selvamani R.
e-mail: selvam1729@gmail.com
ORCID: 0000-0001-5166-5449

Rubine L.
e-mail: rubineloganathan5@gmail.com
ORCID:

Rexy J.
e-mail: rexyallan1@gmail.com
ORCID:

Ebrahimi F.
e-mail: febrahimy@gmail.com
ORCID: 0000-0001-9091-4647